Title: Effect of promoters on Cu-ZnO-SiO_2 catalyst for gas-phase hydrogenation of maleic anhydride to γ-butyrolactone at atmospheric pressure

Author: Yang Yu Yanglong Guo Wangcheng Zhan Yun Guo Yunsong Wang Guanzhong Lu

PII: S1381-1169(14)00177-0
DOI: http://dx.doi.org/doi:10.1016/j.molcata.2014.04.038
Reference: MOLCAA 9101

To appear in: *Journal of Molecular Catalysis A: Chemical*

Received date: 25-2-2014
Revised date: 29-4-2014
Accepted date: 30-4-2014

Please cite this article as: Y. Yu, Y. Guo, W. Zhan, Y. Guo, Y. Wang, G. Lu, Effect of promoters on Cu-ZnO-SiO_2 catalyst for gas-phase hydrogenation of maleic anhydride to *rmgamma*-butyrolactone at atmospheric pressure, *Journal of Molecular Catalysis A: Chemical* (2014), http://dx.doi.org/10.1016/j.molcata.2014.04.038

Effect of promoters on Cu-ZnO-SiO_2 catalyst for gas-phase hydrogenation of maleic anhydride to γ-butyrolactone at atmospheric pressure

Yang Yu, Yanglong Guo*, Wangcheng Zhan, Yun Guo, Yunsong Wang, Guanzhong Lu*

Key Laboratory for Advanced Materials, Research Institute of Industrial Catalysis, East China University of Science and Technology, Shanghai 200237, P. R. China

ABSTRACT

Cu-ZnO-SiO_2 (CZS) catalysts, prepared by the coprecipitation method, were investigated for gas-phase hydrogenation of maleic anhydride (MA) to γ-butyrolactone (GBL) at atmospheric pressure and characterized by XRD, N_2O chemisorption, SEM and TGA. Effects of the compositions and the promoters on the catalytic performance and stability of CZS catalysts were investigated, in which CZS111 catalyst with the molar ratio of Cu:Zn:Si=1:1:1 showed better catalytic performance and stability. The results show that the introduction of Ba as a promoter to CZS111 catalyst can further improve greatly the catalyst stability by increasing Cu surface area and ZnO dispersion with more additional adsorption sites for succinic anhydride (SA) to suppress the adsorption and polymerization of SA on the active sites of Cu^0. The possible reaction pathways were proposed for gas-phase hydrogenation of MA to GBL, which could explain well the effect of Ba as a promoter on the stability of CZS111 catalyst.

Keywords: Maleic anhydride; γ-Butyrolactone; Gas-phase hydrogenation; Cu-ZnO-SiO_2 catalyst; promoter

* Corresponding authors. Fax: +86 21 64252923. E-mail addresses: ylguo@ecust.edu.cn (Y. Guo), gzhlu@ecust.edu.cn (G. Lu).

1. Introduction

Many researches focus on syntheis of γ-butyrolactone (GBL) due to its versatile applications. For instance, GBL is used largely as a solvent of polyethylene, polyvinyl chloride and polystyrene, and as an extracting agent of aromatic hydrocarbon, water-immiscible ethanol and cyclic ether. GBL, with oxygen-containing five-membered molecular structure, is an important intermediate for synthesis of N-methylpyrrolidone [1], N-vinylpyrrolidone [2], and some medicines [3, 4]. Furthermore, GBL can also serve as the cell electrolyte solvent instead of the strong corrosion acid liquid [5, 6].

The production of GBL mainly includes two processes, i.e., dehydrogenation and cyclization of 1, 4-butanediol (BDL) [7, 8] and direct hydrogenation of maleic anhydride (MA). The direct hydrogenation of MA to GBL is an economically promising process due to the availability of low-price MA from the large-scale industrialization of the partial oxidation of n-butane to MA.

Some works were reported on the direct hydrogenation of MA to GBL in gas phase, liquid phase, or supercritical CO_2. The latter two processes were carried out preferably over noble metal catalysts, such as Pd-MoO_x-NiO/SiO_2 [9], Pd/SiO_2 [10], Pd-SnO_2/SiO_2 [11], Ru complexes [12, 13], and Pd/Al_2O_3 [14], Pd/C [15, 16] under higher reaction pressures. However, gas-phase hydrogenation of MA to GBL at atmospheric pressure over transition metal catalysts is a better choice because of mild reaction conditions and low-cost catalysts. Some transition metal catalysts were reported with good catalytic performance for gas-phase hydrogenation of MA to GBL at atmospheric pressure, such as Cu-ZnO-Al_2O_3 [17], Cu-ZnO-TiO_2 [18], Cu-ZnO-ZrO_2 [19], Cu-ZnO-CeO_2 [20], Cu-TiO_2-Al_2O_3 [21], Cu/metal oxides (Al_2O_3, ZrO_2 or ZnO) [22], Ni or Co/SiO_2 [23], Ni/SiO_2, /SiO_2-Al_2O_3 or /H-BEA [24, 25], ect, in which Cu-based catalysts have better catalytic performance, especially the selectivity to GBL. Most works of Cu-based catalysts focus on the structure-activity relationship, however,

the stability of Cu-based catalysts and how to improve the catalyst stability have been rarely reported.

According to our previous study [26], the deactivation of Cu-based catalyst for gas-phase hydrogenation of maleic anhdyride to γ-butyrolactone was mainly attributed to the formation of carbonaceous species on the catalyst surface. To retard generation of surface carbonaceous species and improve the stability of Cu-based catalyst for the hydrogenation reactions, neutral SiO_2 support was usually selected as a substitute for acidic supports, such as Al_2O_3 support. Moreover, Garetto *et al.* [27] investigated gas-phase hydrogenation of MA over Cu/SiO_2 catalyst and derived a deactivation model with residual activity, in which high conversion of MA and selectivity to succinic anhydride (SA) were obtained, whereas the yield of GBL was always lower than 2~3 %. In this work, Cu-ZnO-SiO_2 (CZS) catalysts, prepared by the coprecipitation method, were investigated for gas-phase hydrogenation of MA to GBL at atmospheric pressure. Effects of the compositions and the promoters on the catalytic performance and stability of CZS catalysts were also investigated, and the possible reaction pathways for gas-phase hydrogenation of MA to GBL at atmospheric pressure were proposed.

2. Experimental

2.1. Preparation of catalyst

CZS and CZS+P (P = Mg, Ca, Ba, Ce, Co, Cr or Fe) catalysts were prepared by the coprecipitation method with 1.0 mol·L^{-1} Na_2CO_3 aqueous solution as precipitating agent. The nitrates of copper, zinc and P (P:Cu=1:10, molar ratio) with the given molar ratios were dissolved in deionized water to obtain 0.5 mol·L^{-1} aqueous solution, and then the precipitating agent was added dropwise into the nitrates solution under vigorous stirring at room temperature until pH≈8. After being aged for 0.5 h under gentle stirring, the precipitate was washed thoroughly by deionized water to remove residual Na^+ and followed by vacuum

filtration. Then the resultant precipitate was dispersed in 200 mL of absolute ethanol under vigorous stirring to form a suspension at 60 ^{o}C in oil bath, and then a certain quantity of silica sol with 10 wt.% SiO_2 was added dropwise into the suspension. The final precipitate was aged for 0.5 h, filtrated in vacuum, dried at 120 ^{o}C overnight and calcined in air at 450 ^{o}C for 4 h. At last, the as-prepared catalyst was pressed and then crushed into 20~40 mesh particles for evaluation of its catalytic performance. The compositions and physicochemical properties of CZS catalysts are shown in Table 1.

Table 1
The compositions and physicochemical properties of CZS catalysts.

Catalysts	Molar ratios			S_{Cu} [a] ($m^2 \cdot g^{-1}$)	D_{Cu} [b] (nm)
	Cu	Zn	Si		
CZS111	1.0	1.0	1.0	9.5	14
CZS1511	1.5	1.0	1.0	8.0	16
CZS211	2.0	1.0	1.0	7.8	17
CZS1151	1.0	1.5	1.0	9.6	12
CZS121	1.0	2.0	1.0	10.0	10
CZS1115	1.0	1.0	1.5	10.3	10
CZS112	1.0	1.0	2.0	10.8	9

[a] Cu surface area of the fresh catalyts; [b] Crystallite size of Cu in the fresh catalysts.

2.2. Test of catalytic performance

Gas-phase hydrogenation of MA to GBL was carried out in a tubular quartz fixed-bed reactor (inside diameter = 13 mm, length = 650 mm) at atmospheric pressure. 6 mL of catalyst (height = 45 mm) was packed in the constant temperature part of the reactor, and then 15 mL of quartz sand pretreated at 600 ^{o}C in air was loaded above the catalyst for the complete gasification of the raw material (20 wt.% MA dissolved in GBL). Prior to the test, the as-prepared catalyst was activated by 60 mL·min^{-1} of 5 vol.% H_2/N_2 at 300 ^{o}C for 6 h (designated as the fresh catalyst). Then the temperature was lowered to 220 ^{o}C, and 27.5 NmL·min^{-1} of pure H_2 and 0.2 h^{-1} (liquid hourly space velocity, LHSV) of raw material, were fed into the reactor. The products were sampled using the conical beakers cooled by an ice-bath at intervals of 1 h and analyzed by Perkin-Elmer Clarus 500 gas chromatograph equipped with a FID detector and a SE-54 capillary column (25 m × 0.32 mm × 1.0 μm). The

temperatures of the injector and detector were 220 ^{o}C, and the temperature of the column oven was kept at 100 ^{o}C for 1 min and then increased programmedly to 120 ^{o}C at the rate of 5 ^{o}C·min^{-1}.

2.3. Characterization of catalyst

The powder XRD patterns were recorded on a Bruker AXS D8 Focus diffractometer operated at 40 kV, 40 mA (Cu Kα radiation, λ=0.15406 nm), and the diffraction patterns were taken in the range of $10^{o}<2\theta<80^{o}$ at the scanning rate of 6 ^{o}·min^{-1}. The Cu surface area of the fresh catalyst was measured by N_2O chemisorption at 60 ^{o}C assuming a molar stoichiometry of Cu:N_2O=2 and a surface atomic density of 1.46×10^{19} Cu atoms·m^{-2} [28]. SEM images were recorded on a JEOL JSM-6360LV scanning electron microscope. TGA profiles were recorded on a PerkinElmer Pyris Diamond TG-DTA analyzers, in which the sample was heated programmedly from 40 to 800 ^{o}C at the rate of 10 ^{o}C·min^{-1} in the atmosphere of air of 100 mL·min^{-1}.

3. Results and discussion

3.1. Catalytic performance of CZS catalyst

Table 2 shows the catalytic performance of CZS catalysts for gas-phase hydrogenation of MA to GBL at atmospheric pressure. Compared with Cu/SiO_2 catalyst for gas-phase hydrogenation of MA [27], the introduction of ZnO to Cu-SiO_2 catalyst considerably enhanced the selectivity to GBL. Taking CZS111 catalyst as a reference, within reaction time of 1 h, an increase in SiO_2 or ZnO content in CZS catalyst led to a slight increase in the conversion of MA and a slight decrease in the selectivity to GBL. However, a reverse variation tendency of the catalytic performance occurred with an increase in Cu content in CZS catalyst. Moreover, few by-products were produced, such as tetrahydrofuran (THF), n-

butylaldehyde (BD) and n-butyric acid (BA).

Over all CZS catalsyts, after reaction for 5 h, the conversion of MA and the selectivity to GBL hardly changed, however, a few amout of SA appeared; after reaction for 10 h, both the conversion of MA and the selectivity to GBL showed a drastic drop, and meanwhile, SA became the only by-product. After reaction for 10 h, the residual catalytic performance of CZS111 catalyst was the highest among all CZS catalysts in terms of the yield of GBL.

Table 2
The catalytic performance of CZS catalysts for gas-phase hydrogenation of MA to GBL at atmospheric pressure.

Catalysts	Molar ratios			MA conversion vs. reaction time (%)			Selectivity vs. reaction time (%)											
							GBL			THF			SA			BD and BA		
	Cu	Zn	Si	1h	5h	10h	1h	5h	10h	1h	5h	10h	1h	5h	10h	1h	5h	10h
CZS111	1.0	1.0	1.0	96.0	96.0	55.0	98.0	98.0	33.0	0.8	0.7	-	-	0.3	67.0	1.2	1.0	-
CZS1511	1.5	1.0	1.0	95.0	95.0	30.0	97.0	97.0	31.0	1.0	0.8	-	-	0.4	69.0	2.0	1.8	-
CZS211	2.0	1.0	1.0	94.0	94.0	35.0	98.6	97.7	16.0	0.6	0.4	-	-	1.7	84.0	0.8	0.2	-
CZS1151	1.0	1.5	1.0	97.6	96.9	20.0	96.8	95.9	21.0	1.2	0.8	-	-	2.6	79.0	2.0	0.7	-
CZS121	1.0	2.0	1.0	98.4	98.4	16.0	95.0	95.0	35.0	2.1	1.7	-	-	0.8	65.0	2.9	2.5	-
CZS1115	1.0	1.0	1.5	98.7	98.2	25.0	93.0	92.7	19.0	3.9	2.5	-	-	2.8	81.0	3.1	2.0	-
CZS112	1.0	1.0	2.0	99.0	98.5	40.0	91.0	90.5	10.0	5.1	3.0	-	-	3.9	90.0	4.0	2.6	-

3.2. Effect of reaction temperature

Table 3 shows the effect of the reaction temperature on the catalytic performance of CZS111 catalsyt. At the same reaction time, with an increase in reaction temperature, the relationship between the conversion of MA and the reaction temperature displayed a volcano shape correlation, and the highest conversion of MA appeared at the reaction temperature of 260 ºC. However, the selectivity to GBL gradually decreased, which was consistent with Castiglioni et al.'s results [17] that higher reaction temperatures led to the further hydrogenation and/or hydrogenolysis of GBL. Taking the comprehensive performance of CZS111 catalsyt into account, the optimum reaction temperature for gas-phse hydrogenation of MA to GBL over CZS111 catalyst was 220 ºC.

Table 3
The catalytic performance of CZS111 catalyst for gas-phase hydrogenation of MA to GBL at atmospheric pressure at different reaction temperatures.

Reaction temperature (ºC)	MA conversion (%)			Selectivity (%)											
				GBL			THF			SA			BD and BA		
	1h	5h	10h	1h	5h	10h	1h	5h	10h	1h	5h	10h	1h	5h	10h
220	96.0	96.0	55.0	98.0	98.0	33.0	0.8	0.7	-	-	0.3	67.0	1.2	1.0	-
240	96.4	96.5	56.2	97.6	97.5	31.2	1.1	0.9	-	-	0.4	68.8	1.3	1.2	-
260	97.0	97.2	57.6	96.4	96.0	27.6	1.7	1.5	-	-	0.8	72.4	1.9	1.7	-
280	96.5	96.1	55.8	94.8	94.9	24.5	2.8	2.1	-	-	1.1	75.5	2.4	1.9	-

3.3. Effect of promoters

CZS111 catalyst showed better catalytic performance for gas-phase hydrogenation of MA to GBL at atmospheric pressure. However, the catalyst stability was unsatisfactory. To improve the stability of CZS111 catalyst, several promoters (P = Mg, Ca, Ba, Ce, Co, Cr and Fe) were investigated. The physicochemical properties of CZS111+P catalsyts are shown in Table 4.

Table 4
The physicochemical properties of CZS111+P catalysts.

Catalysts	S_{Cu} ($m^2 \cdot g^{-1}$)	D_{Cu} (nm)	D_{ZnO} [a] (nm)
CZS111	9.5	14	15
CZS111+Ba	15.9	10	9
CZS111+Mg	10.4	12	13
CZS111+Ca	10.7	12	10
CZS111+Ce	12.6	9	11
CZS111+Co	8.2	13	14
CZS111+Cr	10.2	12	9
CZS111+Fe	7.6	13	13

[a] The crystallite size of ZnO in the fresh CZS111+P catalysts determined by Scherrer's equation using the diffraction peak of ZnO (101).

Fig. 1 shows the catalytic performance of CZS111+P catalysts for gas-phase hydrogenation of MA to GBL at atmospheric pressure, in which the selectivities to byproducts, such as SA, THF, BD or BA, are not shown. As shown in the inset at the lower left corner of Fig. 1, the introduction of Mg, Ca, Co or Fe decreased the catalytic activity of CZS111 catalyst. The introduction of Cr led to a slight increase in the catalytic activity. However, the Ce- or Ba-promoted CZS111 catalyst had an obvious increase in the catalytic activity, in which the

conversion of MA could reach 100% over CZS111+Ce catalyst and 97.8% over CZS111+Ba catalyst, respectively. As for the selectivity, as shown in the inset at the upper right corner of Fig. 1, the introduction of Ce or Ba to CZS111 catalyst could also increase the selectivity to GBL. Most importantly, with the introduction of Ba to CZS111 catalyst, the decline rates of the catalytic activity and the selectivity to GBL were both suppressed to a great extent. After reaction for 10 h, 90.0% of the conversion of MA and 69.8% of the selectivity to GBL remained over CZS111+Ba, whereas the corresponding percentages were only 55.0% and 33.0% over CZS111 catalyst at the same reaction time, respectively.

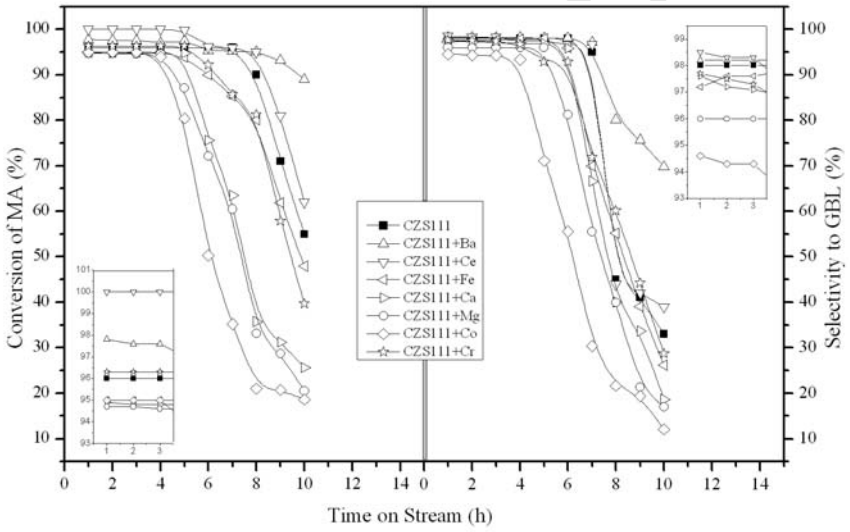

Fig. 1. The catalytic performance of CZS111+P catalysts for gas-phase hydrogenation of MA to GBL at atmospheric pressure.

To further investigate the effect of a promoter on the catalytic stability of CZS111 catalyst, the stability tests for 50 h were carried out and the results are shown in Fig. 2. The catalytic performance of CZS111 catalyst and three representative CZS111+P (Ba, Ce, Mg) catalysts gradually declined and then reached a steady state after reaction for about 22 h. The conversion of MA and selectivity to GBL of CZS111+Ba catalyst and CZS111 catalyst after reaction for 50 h were 59.1%/35.8% and 33.9%/11.7%, respectively.

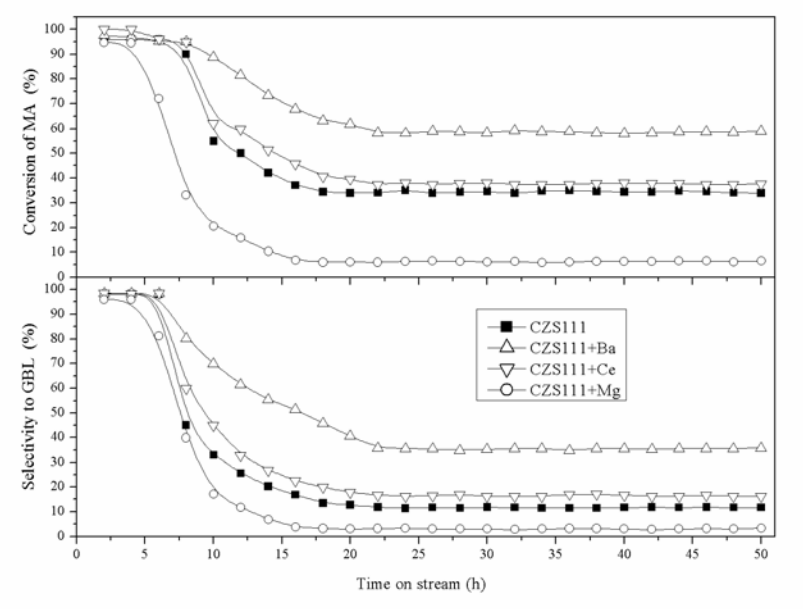

Fig. 2. The catalytic stability of CZS111 and three representative CZS111+P catalysts for gas-phase hydrogenation of MA to GBL at atmospheric pressure.

3.4. Characterization of catalyst

Fig. 3 shows XRD patterns of the as-prepared and the fresh CZS catalysts. As shown in Fig. 2, XRD patterns of all as-prepared CZS catalysts exhibited well-resolved characteristic diffraction peaks of CuO (PDF#65-2309) and ZnO (PDF#36-1451), respectively. Three characteristic diffraction peaks of Cu (PDF#65-9743) located at 2θ=43.4^o, 50.6^o and 74.3^o, corresponding to the crystal planes of Cu (111), (200) and (220), respectively, and the characteristic diffraction preaks of ZnO were identified in XRD patterns of all fresh CZS catalysts. It indicated that CuO was completely reduced by 5 vol.% H_2/N_2 to Cu^0 and the state of ZnO did not change, in which Cu^0 is the active site for gas-phase hydrogenation of MA to GBL [18-20, 26]. In all XRD patterns, a very broad peak in the 2θ range from 15^o to 30^o should be assigned to the characteristic diffraction peak of amorphous SiO_2 [29]. The crystallite size of Cu in the fresh CZS catalysts, calculated by Scherrer's equation with the full peak width at half maximum height of the characteristic diffraction of Cu (111), is shown in

Table 1. As shown in Table 1, the crystallite size of Cu decreased with an increase in ZnO or SiO_2 content in CZS catalysts. Combined with the catalytic performance shown in Table 2, there was a correlation between the catalytic performance and the crystallite size of Cu over CZS catalyst for gas-phase hydrogenation of MA to GBL, in which with a decrease in the crystallite size of Cu, the conversion of MA increased but the selectivity to GBL decreased.

Fig. 4 shows XRD patterns of the as-prepared and the fresh CZS111+P catalysts. Similar to CZS catalysts, after reduced by 5 vol.% H_2/N_2, CuO in the as-prepared CZS111+P catalyst was completely reduced to Cu^0 and ZnO remained. Except for a characteristic diffraction peak of CeO_2 at 2θ = 28.5° in XRD pattern of CZS111+Ce catalyst, no characteristic diffraction peaks related to the promoters were observed in XRD patterns of other CZS111+P catalysts. Table 4 shows the crystallite size of Cu in the fresh CZS111+P catalysts. As shown in Table 3, the introduction of the promoters could decrease the crystallite size of Cu in CZS111 catalyst, especially the introduction of Ba or Ce.

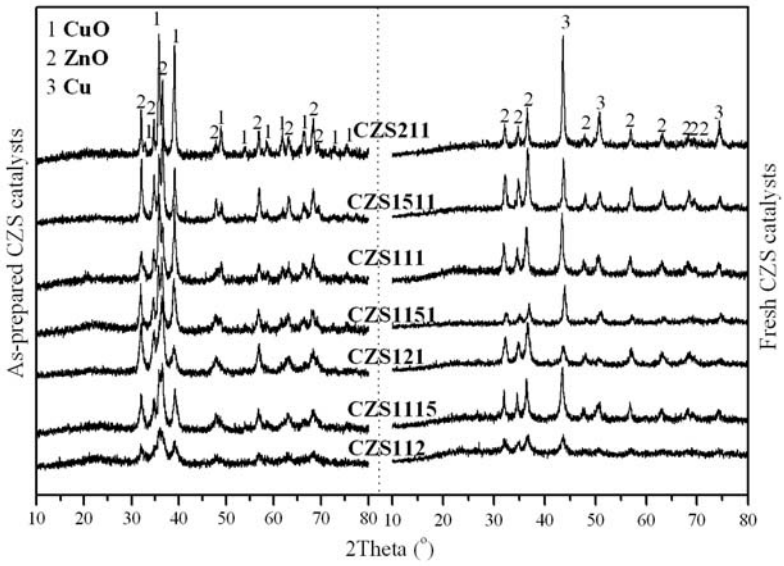

Fig. 3. XRD patterns of the as-prepared and the fresh CZS catalysts.

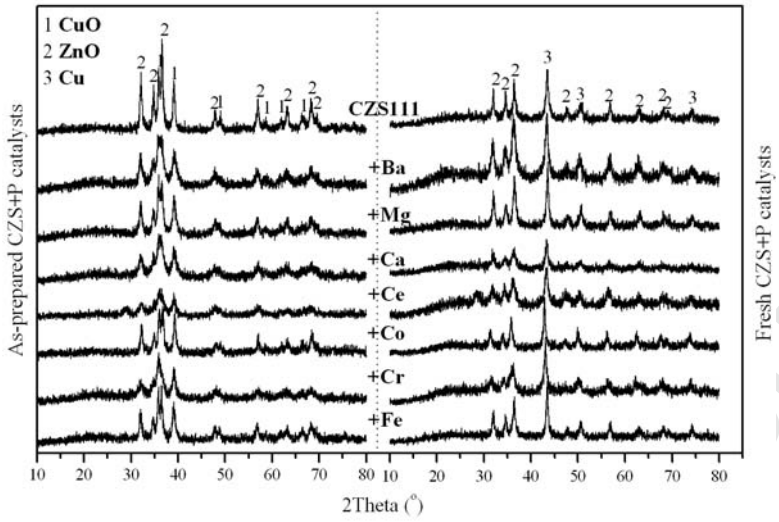

Fig. 4. XRD patterns of the as-prepared and the fresh CZS111+P catalysts.

The Cu surface area (S_{Cu}), a measure indicative of the quantity of exposed Cu atmos per gram of catalyst, is a significant parameter in the hydrogenation reaction over Cu-based catalysts [30]. According to S_{Cu} data shown in Table 1 and Table 4, compared with CZS111 catalyst, with an increase in Cu content in CZS catalyst, S_{Cu} decreased. However, with an increase in ZnO or SiO_2 content in CZS catalyst, S_{Cu} had a slight increase. S_{Cu} of CZS111+P catalysts were affected by the introduction of the promoters. Co or Fe as promoter led to a decrease in S_{Cu}, but Mg, Ca or Cr as promoter resulted in a slight increase in S_{Cu}. In particular, with the introduction of Ba or Ce to CZS111 catalyst, the corresponding S_{Cu} increased by 6.4 and 3.1 $m^2 \cdot g^{-1}$ than that of CZS111 catalyst, respectively. Combined with the catalytic performances of CZS111+P catalysts shown in Fig. 1 and 2, it indicates that S_{Cu} is an important parameter for screening a better Cu-based catalyst for gas-phase hydrogenation of MA to GBL at atmospheric pressure, especially taking the catalyst stability into consideration.

The surface morphologies of the fresh and the used CZS111 catalysts were investigated by SEM. As shown in Fig. 5, it was bright and clean on the surface of the fresh CZS111 catalyst. However, with an increase in the reaction time, some fuscous cotton-like deposition appeared

on the catalyst surface and gradually covered most of the surface. It indicates that the deactivation of CZS111 catalyst mainly results from formation of the surface deposition, which covers the active sites of Cu^0.

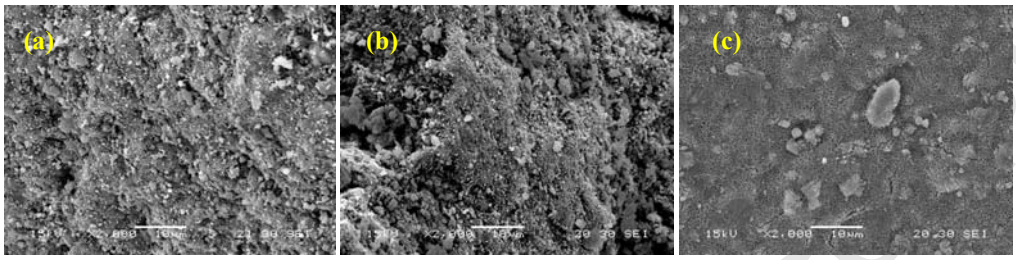

Fig. 5. SEM images of the fresh CZS111 catalyst (a), the used CZS111 catalyst for reaction for 10 h (b) and the used CZS111 catalyst for reaction for 50 h (c).

After reaction for 10 h, the contents of the surface deposition over used CZS111 and CZS111+Ba catalysts were determined by TGA. As shown in Fig. 6, the weight loss ($\triangle_{wt}$) of the used CZS111+Ba catalyst was lower than that of the used CZS111 catalyst, which indicates that the introduction of Ba to CZS111 catalyst reduces the formation rate of the surface deposition over the catalyst and thus improves the catalyst stability.

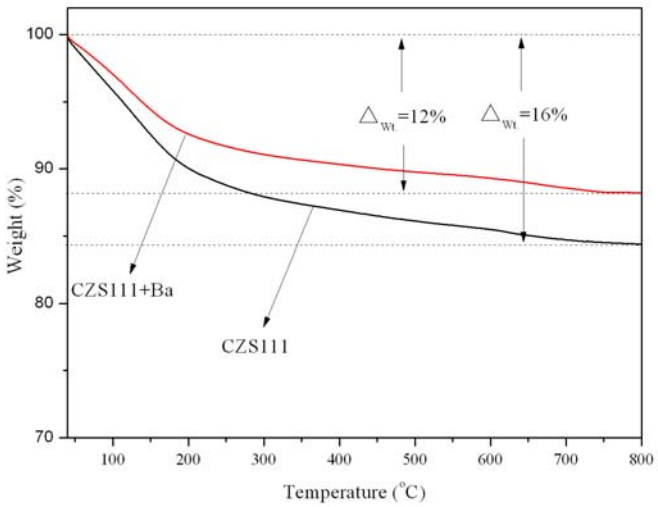

Fig. 6. TGA profiles of the used CZS111 and CZS111+Ba catalysts.

3.5. The reaction pathways over CZS111 and CZS111+Ba catalysts

Table 2 shows that the selectivity to SA, as a transition species in the catalytic hydrogenation of MA to GBL [10], rapidly increased when CZS111 catalyst started to deactivate after reaction for several hours, and at the same time, the selectivity to GBL decreased. It indicates that SA can not be hydrogenated to GBL promptly and is strongly adsorbed then polymerized on the catalysts surface, which results in the fast deactivation of the catalyst [26]. Herrmann *et al*. [31] and Emig *et al*. [32] investigated the effect of ZnO over Cu-based catalysts in the catalytic hydrogenation of MA and proposed that ZnO without catalytic activity could provide the additional adsorption sites for SA to alleviate the competitive adsorption of GBL and SA on the active sites of Cu^0. In this work, the introduction of Ba could significantly increase the Cu surface area of CZS111 catalyst. Meanwhile, ZnO was also highly dispersed, as implied by its smaller crystallite size shown in Table 4, that was to say, ZnO could provide more adsorption sites for SA, which could alleviate the adsorption and polymerization of SA on the active sites of Cu^0 and thus improved the stability of CZS111 catalyst.

The reaction pathways for gas-phase hydrogenatio of MA to GBL at atmospheric pressure over CZS111+Ba (a) and CZS111 (b) catalysts were proposed in Scheme 1. First, the gasified MA in the flow of hydrogen diffused to the catalyst surface and started to react in the sequence of (1)~(3) on the active sites of Cu^0 of the catalyst surface. It was different from the results reported by Emig *et al*. [32] that no 1, 4-butanediol was produced over CZS or CZS111+Ba catalysts in reaction (3). Reaction (1) is a quick process over a catalyst [14]. Initially, except that some SA were reversibly adsorbed on the adjacent ZnO surface, most of SA were hydrogenated to GBL (2). With the reaction progressing, more SA were produced. The excessive SA were strongly adsorbed and then polymerized on the active sites of Cu^0 (4). Meanwhile, based on the competitive adsorption between GBL and SA on the active sites of Cu^0, reaction (3) was suppressed to a certain extent, which led to a decrease in the selectivity to by-products, such as THF, BA and BD. Compared with CZS111 catalyst (b), the

introduction of Ba (a) could increase Cu surface area and ZnO dispersion with more additional adsorption sites for SA, which decreased the rate of SA polymerization on the active sites of Cu^0 and thus improved the stability of CZS111 catayst.

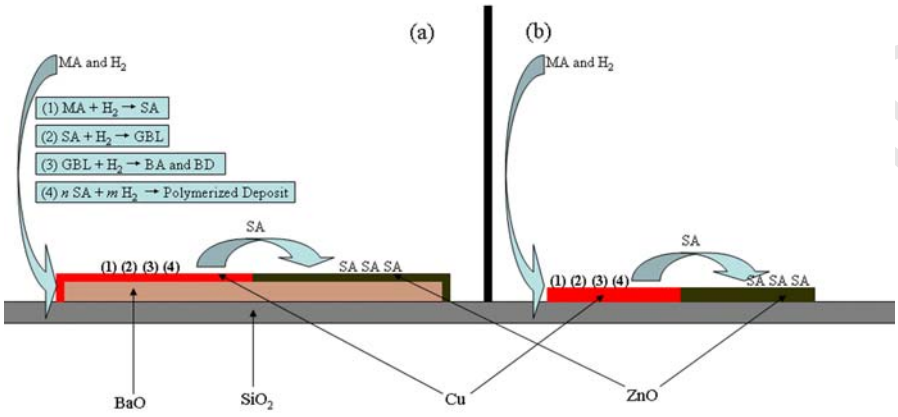

Scheme 1. The reaction pathways proposed for gas-phase hydrogenation of MA to GBL over CZS and CZS111+Ba catalysts at atmospheric pressure.

4. Conclusions

CZS catalysts with different compositions were investigated for gas-phase hydrogenation of MA to GBL at atmospheric pressure. CZS catalysts showed better catalytic performance, in which CZS111 catalyst showed better stability. Effects of promoters on the catalytic performance of CZS111 catalysts were also investigated, in which Ba or Ce as a promoter was favorable for increasing the catalytic performance of CZS111 catalyst. In particular, the introduction of Ba as a promoter to CZS111 catalyst could significantly improve the catalyst stability by increasing Cu surface area and ZnO dispersion.

The possible reaction pathways were proposed for gas-phase hydrogenation of MA to GBL at atmospheric pressure over CZS111 and CZS111+Ba catalysts, which could explain well the effect of Ba as a promoter on the stability of CZS111 catalyst.

Acknowledgements

This project was supported by National Basic Research Program of China (2013CB933201,

2010CB732300), Program for New Century Excellent Talents in University (NCET-09-0343), Shu Guang Project of Shanghai Municipal Education Commission and Shanghai Education Development Foundation (10SG30).

References

[1] Y.S. Yoon, H.K. Shin, B.S. Kwak, Catal. Commun. 3 (2002) 349-355.

[2] Y. Shimasaki, H. Yano, H. Sugiura, H. Kambe, Bull. Chem. Soc. Jpn. 81(2008) 449-459.

[3] S.U. Choi, M.K. Kim, H.S. Ha, Y.I. Hwang, Biotechnol. Lett. 30 (2008) 891-897.

[4] S.L. Kitson, S. Jones, W. Watters, F. Chan, D. Madge, J. Labelled Compd. Rad. 53 (2010) 140-146.

[5] J.Y. Huang, X.J. Liu, X.L. Kang, Z.X. Yu, T.T. Xu, W.H. Qiu, J. Power Sources 189 (2009) 458-461.

[6] S.S. Zhang, D. Foster, J. Read, J. Power Sources 188 (2009) 532-537.

[7] J. Huang, W.L. Dai, K.N. Fan, J. Catal., 266 (2009) 228-235.

[8] B. Zhang, Y.L. Zhu, G.Q. Ding, H.Y. Zheng, Y.W. Li, Appl. Catal. A 443-444 (2012) 191-201.

[9] H. Jeong, T.H. Kim, K.I. Kim, S.H. Cho, Fuel Process. Technol. 87 (2006) 497-503.

[10] S.M. Jung, E. Godard, S.Y. Jung, K.C. Park, J.U. Choi, J. Mol. Catal. A: Chem. 198 (2003) 297-302.

[11] S.M. Jung, E. Godard, S.Y. Jung, K.C. Park, J.U. Choi, Catal. Today 87 (2003) 171-177.

[12] Q. Wang, H.Y. Cheng, R.X. Liu, J.M. Hao, Y.C. Yu, S.X. Cai, F.Y. Zhao, Catal. Commun. 10 (2009) 592-595.

[13] U.R. Pillai, E.S. Demessie, D. Young, Appl. Catal. B 43 (2003) 131-138.

[14] Y. Hara, H. Kusaka, H. Inagaki, K. Takahashi, K. Wada, J. Catal. 194 (2000) 188-197.

[15] U. Herrmann, G. Emig, Ind. Eng. Chem. Res. 36 (1997) 2885-2896.

[16] Q. Wang, H.Y. Cheng, R.X. Liu, J.M. Hao, Y.C. Yu, F.Y. Zhao, Catal. Today 148 (2009) 368-372.

[17] G.L. Castiglioni, M. Ferrari, A. Guercio, A. Vaccair, R. Lancia, C. Fumagalli, Catal. Today 27 (1996) 181-186.

[18] T.J. Hu, H.B. Yin, R.C. Zhang, H.X. Wu, T.S. Jiang, Y.J. Wada, Catal. Commun. 8 (2007) 193-199.

[19] D.Z. Zhang, H.B. Yin, C. Ge, J.J. Xue, T.S. Jiang, L.B. Yu, Y.T. Shen, J. Ind. Eng. Chem. 15 (2009) 537-543.

[20] D.Z. Zhang, H.B. Yin, R.C. Zhang, J.J. Xue, T.S. Jiang, Catal. Lett. 122 (2008) 176-182.

[21] W.J. Lu, G.Z. Lu, G.L. Lu, Y.L. Guo, J.S. Wang, Y. Guo, Chin. J. Catal. 23 (2002) 408-412.

[22] D.Z. Gao, Y.H. Feng, H.B. Yin, A. Wang, T.S. Jiang, Chem. Eng. J. 233 (2013) 349-359.

[23] C.I. Meyer, S.A. Regenhardt, A.J. Marchi, T.F. Garetto, Appl. Catal. A 417-418 (2012) 59-65.

[24] S.A. Regenhardt, C.I. Meyer, T.F. Garetto, A.J. Marchi, Appl. Catal. A 449 (2012) 81-87.

[25] C.I. Meyer, S.A. Regenhardt, M. E. Bertone, A.J. Marchi, T.F. Garetto, Catal. Lett. 143 (2013) 1067-1073.

[26] Y. Yu, Y.L. Guo, W.C. Zhan, Y. Guo, Y.Q. Wang, Y.S. Wang, Z.G. Zhang, G.Z. Lu, J. Mol. Catal. A: Chem. 337 (2011) 77-81.

[27] C.I. Meyer, A.J. Marchi, A. Monzon, T.F. Garetto, Appl. Catal. A 367 (2009) 122-129.

[28] X.M. Guo, D.S. Mao, S. Wang, G.S. Wu, G.Z. Lu, Catal. Commun. 10 (2009) 1661-1664.

[29] F.F. Castillon, N. Bodganchikova, S. Fuentes, M. Avalos-Borja, Appl. Catal. A 175 (1998) 55-65.

[30] E.D. Batyrev, J.C. van den Heuvel, J. Bechers, W.P.A. Jansen, H.L. Castricum, J. Catal. 229 (2005) 136-143.

[31] U. Herrmann, G. Emig, Chem. Eng. Technol. 21 (1998) 285-295.

[32] A. Küksal, E. Klemm, G. Emig, Appl. Catal. A 228 (2002) 237-251.

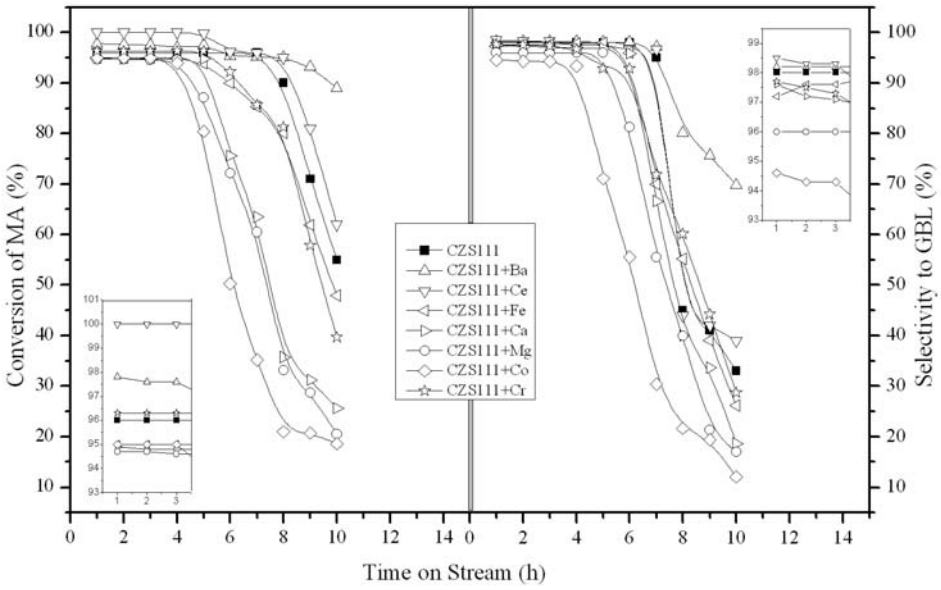

Highlights

Cu-ZnO-SiO_2 catalyst showed better catalytic performance and stability.

Ba as a promoter can further improve greatly the catalyst stability.

Higher Cu surface area and ZnO dispersion can suppress the catalyst deactivation.